

# Molecular Recognition: Use of Metal-Containing Molecular Clefts for Supramolecular Self-Assembly and Host–Guest Formation

James D. Crowley<sup>[a]</sup> and Brice Bosnich<sup>\*[a]</sup>

**Keywords:** Supramolecular / Self-assembly / Host–guest adducts / Molecular cleft receptors / Molecular recognition forces

Molecular clefts consisting of a rigid spacer linked to two parallel cofacially disposed terpy-M–X (M = Pd<sup>2+</sup>, Pt<sup>2+</sup>) units, which can vary in separation from 6.6 to 7.2 Å, have been used as molecular receptors and for self-assembly with linear and triangular linkers to produce rectangles and trigonal prisms, respectively. Aromatic molecules form multiple host–guest adducts with the molecular cleft receptors and with the rectangles and trigonal prisms. Planar complexes of Pt<sup>2+</sup> also

form host–guest adducts. The forces that control this molecular recognition, namely,  $\pi$ – $\pi$  interactions, charge-induced dipole interactions, charge–charge forces, weak metal–metal interactions and solvation effects, are discussed and assigned to the various adducts.

(© Wiley-VCH Verlag GmbH & Co. KGaA, 69451 Weinheim, Germany, 2005)

## Introduction

Fundamental to the functioning of biological systems are the phenomena of molecular recognition and self-assembly. The former relies on the concerted interaction of weak, noncovalent forces<sup>[1]</sup> for selectivity. Generally, the adducts that are formed by weak forces are (kinetically) labile but

can be very (thermodynamically) stable. Self-assembly in biological systems usually involves the use of weak noncovalent forces for the formation of secondary and tertiary structures rather than for the generation of primary sequences of large molecules. The latter usually rely on kinetically controlled covalent bond formation. However, studies in supramolecular chemistry, have generated large complex structures by self-assembly, usually by deploying covalent (metal) coordinate bonds.<sup>[2]</sup> The present review focuses on our studies in molecular recognition and self-assembly using the receptors **1**.<sup>[3]</sup>

[a] Department of Chemistry, The University of Chicago,  
5735 S. Ellis Ave, Chicago, IL 60637, USA  
Fax: +1-773-702-0805  
E-mail: bos5@uchicago.edu

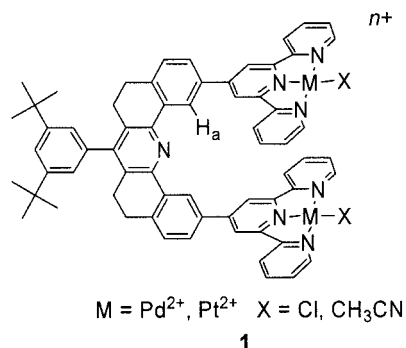


*James D. Crowley was born in “windy” Wellington, New Zealand. He obtained his BSc(Hons) in Chemistry in 1997 and an MSc in 1999 from Victoria University of Wellington. He is currently completing his PhD work under the direction of Professor Brice Bosnich at The University of Chicago. His research interests are in self-assembly, molecular recognition and the development of molecular motors and machines.*



*Brice Bosnich was born in Queensland, Australia. He received his undergraduate degree in the University of Sydney and his Ph.D. in the John Curtin Medical School of the Australian National University, Canberra. He has held posts in University College, London, the University of Toronto and is currently in The University of Chicago. He has worked in the areas of coordination chemistry as well as organometallic chemistry. An underlying theme of his work is the relationship between reactivity and stereochemistry, especially absolute configurations. His current interests are in aspects of supramolecular chemistry, which may be incorporated into the design of molecular switches and motors.*

**MICROREVIEWS:** This feature introduces the readers to the authors' research through a concise overview of the selected topic. Reference to important work from others in the field is included.



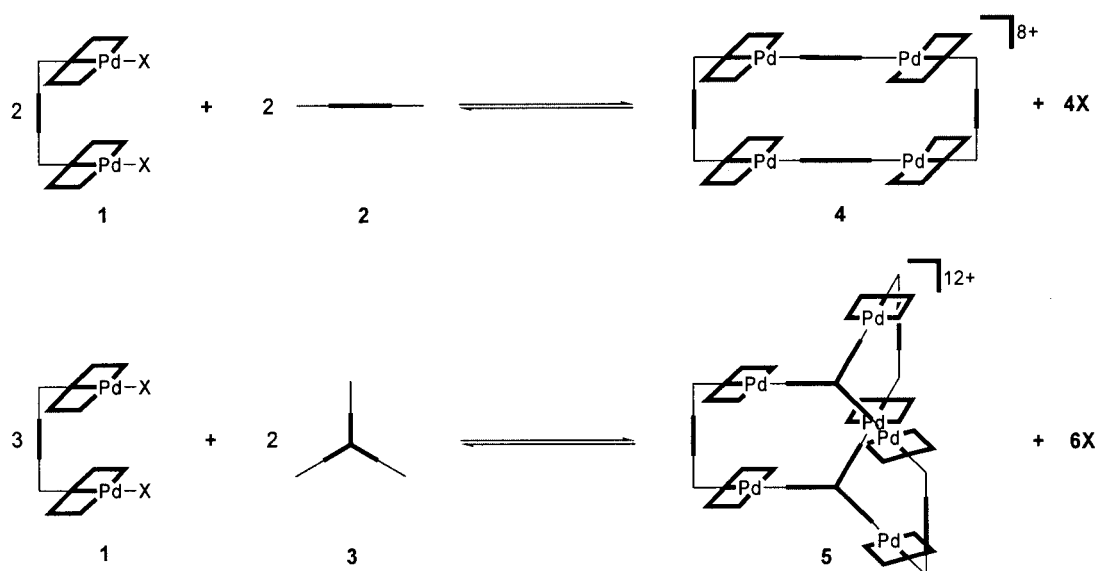
Receptor **1** incorporates the square-planar metals,  $\text{Pd}^{2+}$  or  $\text{Pt}^{2+}$ , and, if  $X = \text{CH}_3\text{CN}$ , this weak ligand is readily displaced. The two terpy-M-X units are parallel to each other and their separation can be modulated by concerted rotation about the spacer while preserving an essentially eclipsed conformation. The terpy-M-X units are charged, are aromatic and, consequently, are expected to incarcerate polarizable aromatic guests, especially those that are negatively charged. The ability of the system to vary the terpy-M-X unit separation allows the receptor to achieve the optimal cleft separation for a particular guest. More complex host structures can be generated from the cleft, **1**, when good leaving groups, X, are present and these clefts are reacted with molecular linkers. Thus linear linkers **2**, or trigonal linkers **3** can provide molecular rectangles **4** or molecular trigonal prisms **5**, respectively.

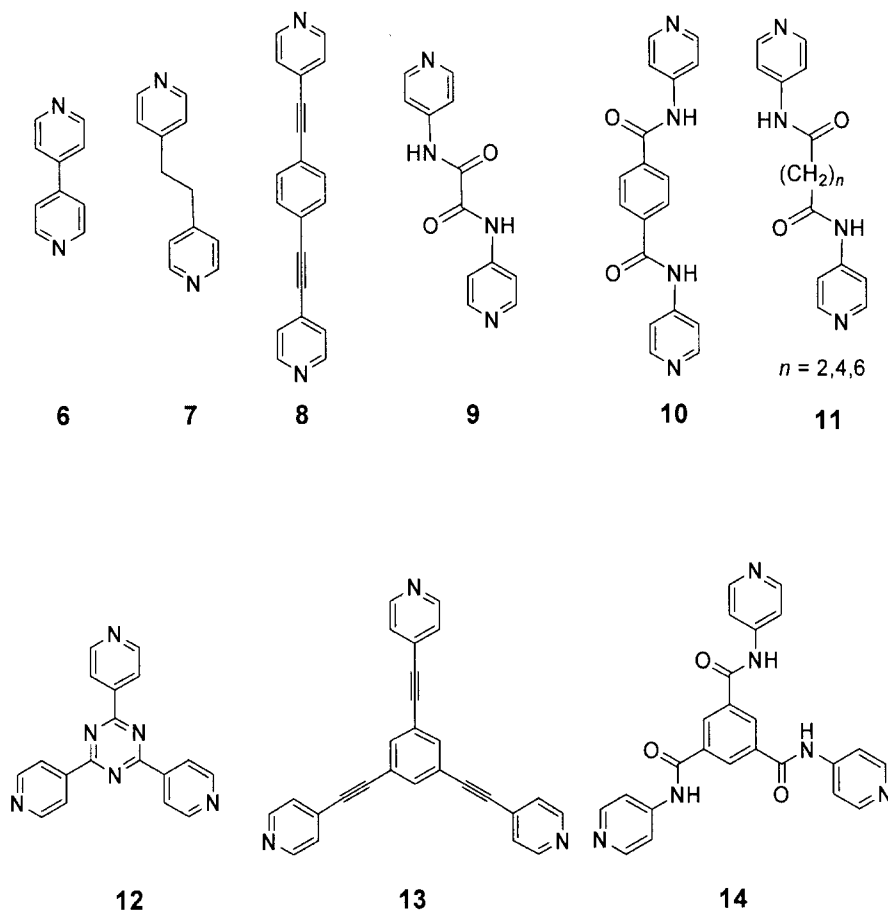
**Self-Assembly:** It is well known that  $\text{Pd}^{2+}$  complexes are more kinetically labile and thermodynamically less stable than the analogous  $\text{Pt}^{2+}$  complexes. As a consequence the ligands of  $\text{Pd}^{2+}$  complexes are substituted more readily than analogous ligands of corresponding  $\text{Pt}^{2+}$  complexes. The relative substitution rates are such that, generally,  $\text{Pd}^{2+}$

complexes are readily substituted at ambient temperatures whereas  $\text{Pt}^{2+}$  complexes require higher temperatures to achieve equivalent rates. Thus, whereas the  $\text{Pd}^{2+}$  complexes have moderate kinetic lability, those of  $\text{Pt}^{2+}$  are kinetically stable at room temperature.<sup>[4]</sup> Molecular rectangles **4** can be self-assembled exclusively by mixing the  $\text{Pd}^{2+}$  molecular cleft,  $X = \text{CH}_3\text{CN}$ , in acetone or acetonitrile with any of the linear linkers **6** to **10**.<sup>[5]</sup> The isolated yields are essentially quantitative. The  $\text{Pt}^{2+}$  analogues can also be prepared but require a different route and more forcing conditions. The more flexible linkers **11** react with the  $\text{Pd}^{2+}$  receptor cleft **1** to give an equilibrium mixture of the desired rectangle and what, by  $^1\text{H}$  NMR spectroscopy and electrospray MS,<sup>[6]</sup> appears to be a macrocycle where a linker joins the two  $\text{Pd}^{2+}$  atoms of the receptor. Scale molecular models indicate that linkers **7**, **9** and **10** are unlikely to form macrocycles with the receptors. Thus, it appears that molecular rectangles will form exclusively with linear linkers of any practical length provided lengthwise linker rigidity is maintained.

By similar methods the three trigonal linkers **12**, **13** and **14** can be combined with the  $\text{Pd}^{2+}$  receptor to give quantitative yields of the trigonal prisms, **5**.<sup>[7]</sup> Because of the insolubility of the trigonal linkers in common solvents, the self-assembly reaction takes several hours with the  $\text{Pd}^{2+}$  complex. The molecular rectangles **4** and trigonal prisms **5** are distinct from the usual supramolecular structures reported, in that the present structures provide specific binding sites for guests, namely, in the molecular clefts.

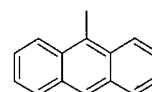
Crystal structures of the free ligand<sup>[8a]</sup> (Figure 1) and that<sup>[8b]</sup> of the  $\text{Pd}^{2+}$  receptor,  $X = \text{Cl}$ , as the  $\text{PF}_6^-$  salt (Figure 2) are shown. The structures are similar in that pairs of molecules interpenetrate one another; in the case of the free ligand, a terpy unit of one molecule lies between two terpy units of another, and a similar structure is obtained for the terpy-Pd-Cl units of the  $\text{Pd}^{2+}$  receptor.





**Host–Guest Adducts:** The  $\text{Pd}^{2+}$  or  $\text{Pt}^{2+}$  receptors **1** ( $\text{X} = \text{Cl}$  or pyridine) form adducts with a variety of guest molecules.<sup>[1]</sup> Included among these are large aromatic molecules especially those that are electron rich and planar neutral or anionic  $\text{Pd}^{2+}$  and  $\text{Pt}^{2+}$  complexes. Although anionic, planar  $\text{Pd}^{2+}$  and  $\text{Pt}^{2+}$  complexes, such as  $[\text{Pd}(\text{dipicolinate})\text{Cl}]^-$  and  $[\text{Pt}(\text{CN})_4]^{2-}$ , appear to form red-colored adducts with the receptors **1**. They are invariably insoluble in all common solvents and are very difficult to characterize. Cationic planar complexes such as  $[\text{M}(\text{terpy})\text{Cl}]^+$ , ( $\text{M} = \text{Pd}^{2+}$ ,  $\text{Pt}^{2+}$ ) do not form adducts with the cationic receptors presumably because of electrostatic repulsion between the positively charged entities. The structure in Figure 2 shows that the cationic terpy-Pd-Cl units can stack on each other in the solid state despite their positive charge. In this case the counterions neutralize the charge repulsion. In solution the receptor shown in Figure 2 shows no evidence of association probably because, as conductivity studies indicate, little or no ion association is present to neutralize the electrostatic repulsion that would ensue upon association.

**Host–Guest Adducts with 9-Methylanthracene:** Both the  $\text{Pd}^{2+}$  and  $\text{Pt}^{2+}$  receptors **1** ( $\text{X} = \text{Cl}$ ), form pale yellow solutions, but upon addition of 9-methylanthracene (**15**), (9-MA), the solutions became deep red, indicative of host–guest formation.

**15**

Using the  $^1\text{H}$  NMR titration mole ratio method (see later),<sup>[9]</sup> it was found that 1:2 host–guest adducts were formed for both the  $\text{Pd}^{2+}$  and the  $\text{Pt}^{2+}$  receptors. The  $\text{Pd}^{2+}$  receptor has microscopic<sup>[10]</sup> stability constants<sup>[3]</sup> of 650 and  $100\text{ M}^{-1}$ , which are similar to those for the  $\text{Pt}^{2+}$  receptor, 800 and  $100\text{ M}^{-1}$ , all constants were obtained in  $\text{CD}_3\text{CN}$  solutions at  $27^\circ\text{C}$ . Nuclear Overhauser ( $^1\text{H}$  ROESY) experiments show<sup>[11]</sup> that one 9-MA guest resides in the molecular cleft, as expected, but that the other 9-MA molecule lies on the outside faces of the terpy-M-Cl units of the receptors. This solution structure obtains in the solid state for the  $\text{Pd}^{2+}$  receptor (Figure 3) where pairs of host–guest molecules stack but each receptor carries two 9-MA guests. As will be seen presently, the 9-MA guest always forms a 1:2 host–guest adduct with the molecular cleft, despite the presence of two sterically equivalent outer faces of the

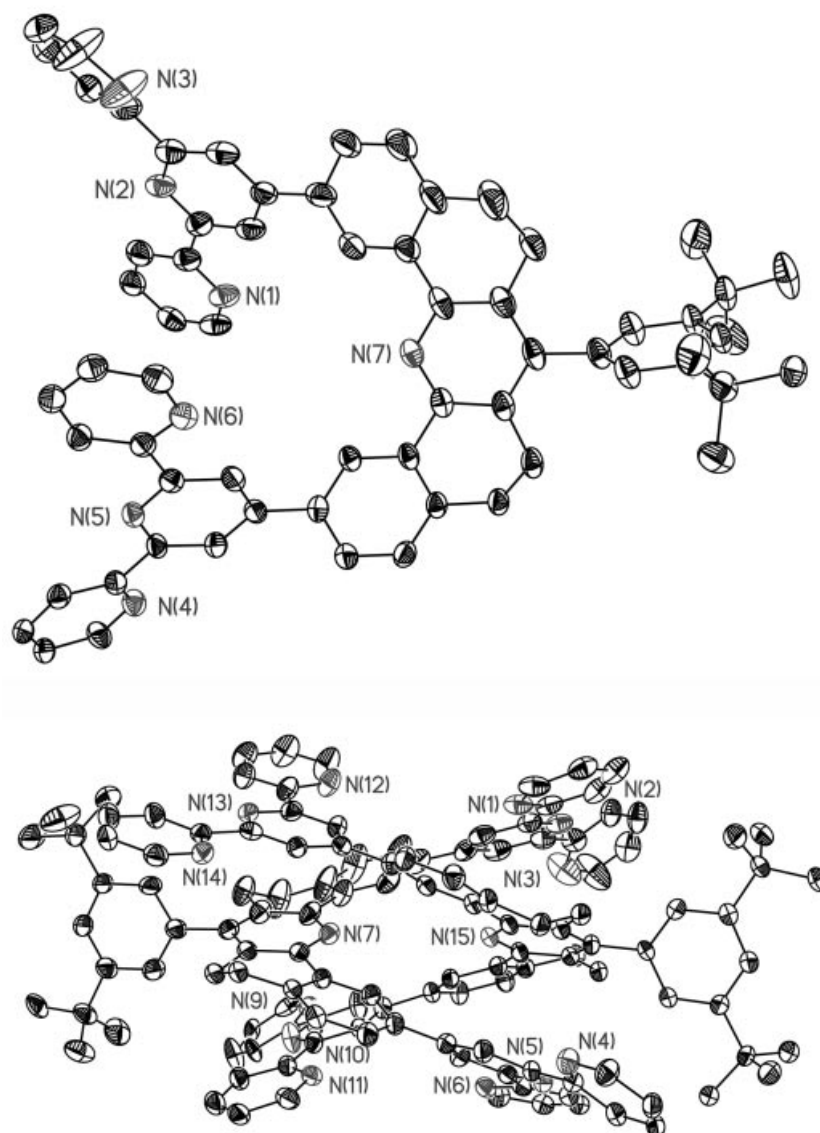


Figure 1. The ORTEP diagram showing a “side” view of the structure that is present in the crystal of the free ligand of **1**. Hydrogen atoms were not located. Thermal ellipsoids are shown at 30% probability. Below, the ORTEP diagram showing the interlocking structure that is present in the crystal of the free ligand of **1**.

terpy-M–X units. However, it is not obvious why 1:3 host–guest adducts are not formed except to suggest that the association of one 9-MA to the outside face of one terpy-M–X unit might lead to electronic polarization of the molecular stack so that the other outer terpy-M–X face is deactivated to association of a 9-MA guest.

The host–guest adducts are very labile. Thus in  $(\text{CD}_3)_2\text{CO}$  solution  $^1\text{H}$  NMR spectra indicate that the 9-MA guests are undergoing rapid inter- and intramolecular exchange even at  $-90^\circ\text{C}$ . We have addressed the question of the rate of intramolecular exchange as well as the preferred occupancy of the 9-MA guest by studying the two molecules **16** and **17**. The intramolecularly tethered anthracene molecule could lie in the cleft as shown in **16**, or it could lie on the outside face of one of the terpy-Pd–Ligand units.

$^1\text{H}$  ROESY spectra show that the anthracene fragment of **16** lies exclusively within the cleft.<sup>[11]</sup> Hence, we conclude that the larger of the two stability constants for the adducts formed with the receptors **1** and free **15** refers to the case of the guest residing in the cleft, as expected.

At  $25^\circ\text{C}$  in  $(\text{CD}_3)_2\text{CO}$  solution the  $^1\text{H}$  NMR spectrum of the system **17** indicates that the two anthracene groups are rapidly exchanging their sites by an intramolecular process.<sup>[11]</sup> As the temperature is lowered, some of the signals first became broad, and then separate into two signals, a process that was complete at  $-90^\circ\text{C}$ . By analyzing this data, it was found that the average residence time (life-time) of the guests in **17** in any site is  $1.6 \times 10^{-5}$  s at  $20^\circ\text{C}$  and 1.3 s at  $-90^\circ\text{C}$ . Because of the intramolecular tethering of the guests, their stability within the respective sites is expected

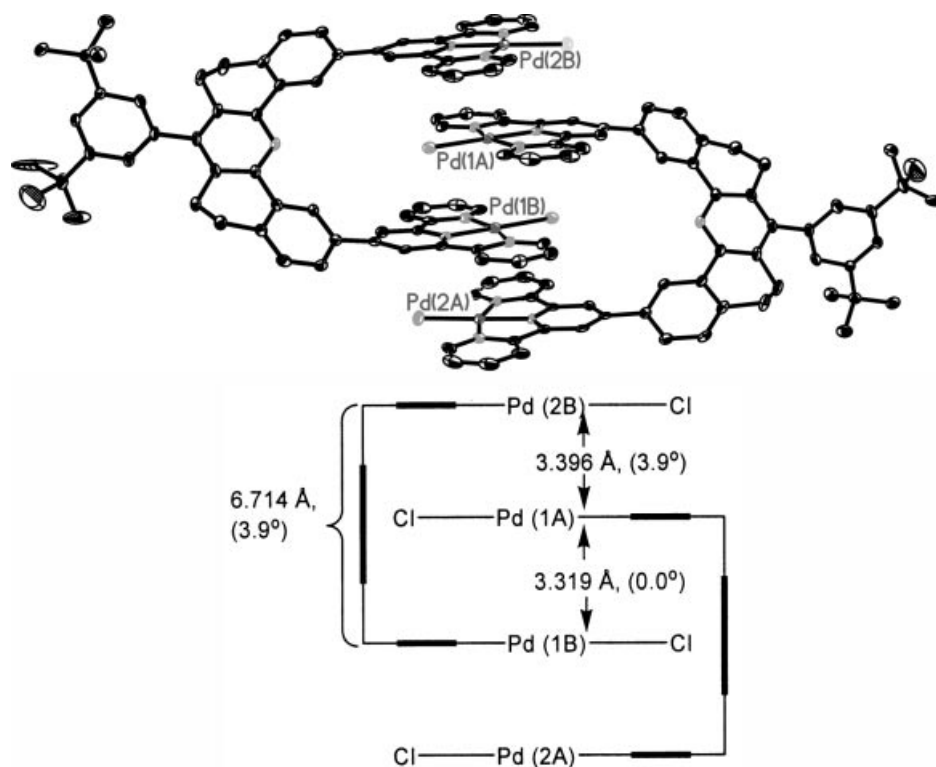


Figure 2. The ORTEP diagram showing a “side” view of the interlocking structure that is present in the crystal of  $[1\text{-Pd}^{2+}(\text{X} = \text{Cl})]^{2+}(\text{PF}_6)_2 \cdot 5\text{CH}_3\text{CN}$ . The solvent and counterions have been removed for clarity. Hydrogen atoms were not located. Thermal ellipsoids are shown at 50% probability. Below, a schematic representation of the important structural details from the crystal structure of the receptor, it is noted that the all the terpy-Pd-Cl unit planes are essentially parallel. The interplanar distances are given and the interplanar angles are shown in brackets.

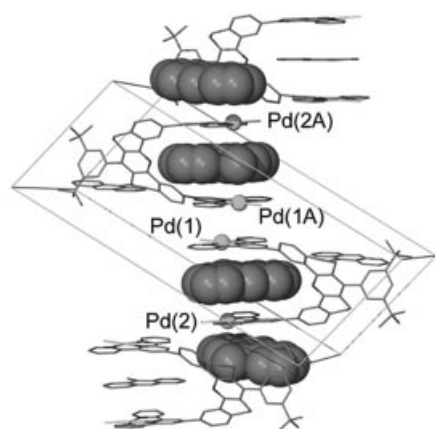


Figure 3. An illustration of the extended crystal structure of  $[1\text{-Pd}^{2+}(\text{X} = \text{Cl})]^{2+}(\text{PF}_6)_2 \cdot 2(9\text{-MA})$ . The box is the unit cell, 9-MA molecules of the stack are shown as space-filling models and the terpy-Pd-Cl units are shown as stick models, as are all other molecules not involved in this stack. Palladium atoms in the stack are shown as spheres.

to be very high, even so, very rapid site exchange occurs. The crystal structure of **17** is shown in Figure 4.

The molecular rectangles **4** derived from **6** and **8**, and the  $\text{Pd}^{2+}$  receptor form 1:4 9-MA host-guest complexes.<sup>[5]</sup>

This is consistent with two 9-MA molecules residing in the two clefts of the rectangle and with the other two guests residing on the (four) outside faces the terpy-Pd-Ligand units, similar to that observed for the single receptors **1**. This site occupancy is supported by the  $^1\text{H}$  NMR spectra chemical shifts of requisite protons of the rectangular receptors. The molecular trigonal prisms **5** behave in a similar manner. The  $\text{Pd}^{2+}$  trigonal prism derived from **12** forms a 1:6 host-guest complex with 9-MA.<sup>[7]</sup> The larger prism formed by the extended linker **13** gives a 1:7 host-guest adduct with 9-MA. Figure 5 shows  $^1\text{H}$  NMR titration plots for the host-guest adducts formed by the smaller and larger trigonal prisms with 9-MA. For the smaller prism, the six 9-MA guests reside in the three clefts and on the (six) outer terpy-Pd-Linker unit faces. The seventh 9-MA molecule is assumed to reside between the two phenyl groups of the linker in the larger prism. Molecular models show that the tritopic guest **18** registers almost exactly with the trigonal prism formed with the larger linker **13**, where each of the three anthracene groups occupies a cleft site. Addition of **18** to a solution of the smaller trigonal prism formed from **12** leads to the destruction of the prism presumably because the guest **18** cannot fit strainlessly within this prism. Such decomposition does not occur in  $[\text{D}_7]\text{dimethylformamide}$  (DMF) solutions at  $70^\circ\text{C}$  with the larger prism formed from **13**. In this case a 1:2 host-guest complex is formed, where one guest **18** lies inside of the prism with each an-



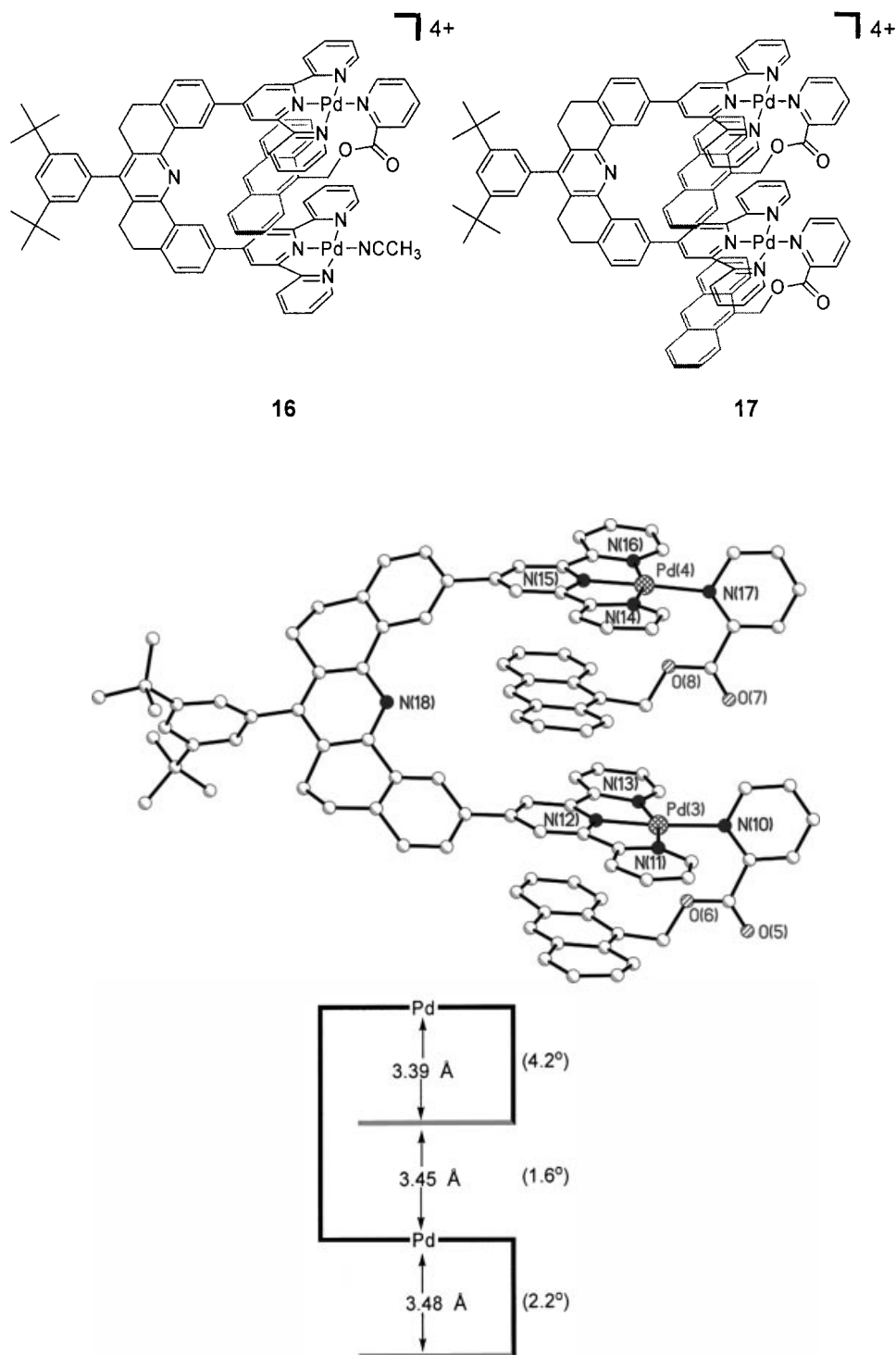


Figure 4. A ball and stick representation of a "side" view for one of the molecules in the unit cell of **17**. Counter ions and solvent molecules have been removed for clarity. Below, a schematic representation of the important structural details from the crystal structure of the **17**. The interplanar distances are given and the interplanar angles are shown in brackets.

thracene group in one of the three clefts, the other guest lies on the "top" and "bottom" faces of the trigonal prism. The host–guest complexes are in rapid intra- and intermolecular exchange.

The host–guest chemistry shown by anthracene derivatives and the molecular clefts **1**, the molecular rectangles **4** and the molecular trigonal prisms **5**, is unexpected in terms of the number of guests that can be incorporated in these

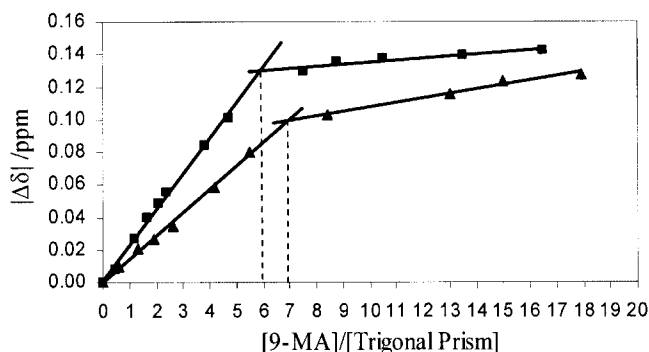
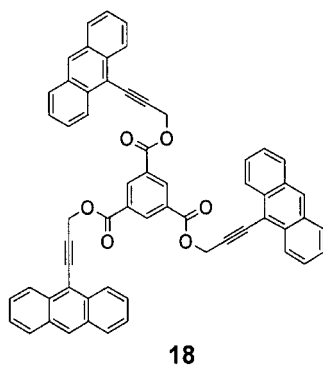


Figure 5.  $^1\text{H}$  NMR chemical shift difference ( $\Delta\delta$ ) stoichiometry plots for the titration of 9-MA with 4 mM solutions of the trigonal prisms derived from **1** and **12** (■) and **1** and **13** (▲). The experiments were performed at 27 °C in  $[\text{D}_7]\text{DMF}$ . The plot refers to the proton  $\text{H}_a$  (see, **1**).



receptors. Furthermore, the host–guest chemistry that obtains for the rectangles and trigonal prisms is different from that usually studied where only one single cavity is present. In the present cases, several cavity sites are presented for host–guest formation.

**Host–Guest Adducts with Planar Metal Complexes:** Magnus' Green Salt<sup>[12]</sup>  $[\text{Pt}(\text{NH}_3)_4][\text{PtCl}_4]$  has long been recognized as the first discovered member of a series of systems containing weak Pt–Pt bonds.<sup>[13]</sup> Whereas  $[\text{Pt}(\text{NH}_3)_4]^{2+}$  is very pale yellow and  $[\text{PtCl}_4]^{2-}$  is salmon pink, the green color of Magnus' salt is due to electronic transitions between the states that arise from Pt–Pt bonding.<sup>[14]</sup> We were interested in determining if weak Pt–Pt (or Pt–Pd) bonds could be used for molecular recognition. The neutral complex **19** was used as a potential guest for both the  $\text{Pd}^{2+}$  and  $\text{Pt}^{2+}$  receptors **1** ( $\text{X} = \text{Cl}$ ).<sup>[13]</sup> The guest **19** forms very stable 1:1 adducts with both the  $\text{Pd}^{2+}$  and  $\text{Pt}^{2+}$  receptors. At 70 °C in  $\text{CD}_3\text{CN}$  solutions, it was found that the stability constants for the  $\text{Pd}^{2+}$  and  $\text{Pt}^{2+}$  receptors are  $12000\text{ M}^{-1}$  and  $51000\text{ M}^{-1}$ , respectively.  $^1\text{H}$  NOE spectroscopy of these two adducts shows that the guest **19** lies in the molecular cleft in both cases.<sup>[15]</sup> The solid-state structure of the **1**– $\text{Pt}^{2+}$ ·**19** adduct ( $\text{X} = \text{Cl}$ ) is shown in Figure 6, where the Pt–Pt distances are 3.303 and 3.262 Å, indicating substantial Pt–Pt interaction.<sup>[13]</sup> Thus, it is likely that weak metal–metal bonding contributes to host–guest stability.

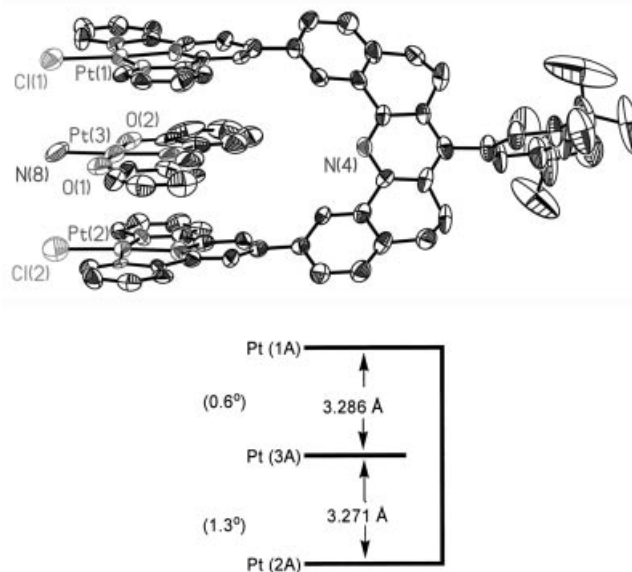
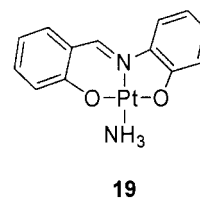
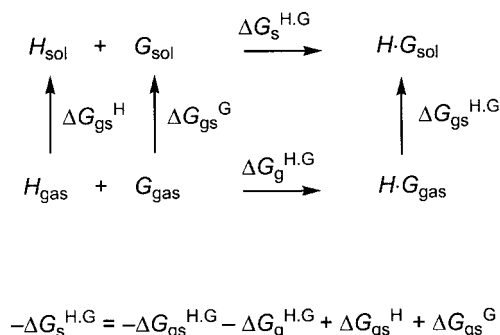


Figure 6. The ORTEP diagram showing a “side” view of the host–guest adduct formed between  $[\text{1-Pt}^{2+}(\text{X} = \text{Cl})]^{2+}(\text{SbF}_6)_2$  and **19**. The solvent and counterions have been removed for clarity. Hydrogen atoms were not located. Thermal ellipsoids are shown at 50% probability. Below, a schematic representation of the important structural details from the crystal structure of the host–guest adduct. The interplanar distances are given and the interplanar angles are shown in brackets.

**Solvent Effects:** The stability of these adducts depends on the solvent employed. The same host–guest adduct stability constants in  $[\text{D}_7]\text{DMF}$  at 70 °C are an order of magnitude smaller than in  $\text{CD}_3\text{CN}$  solution at 70 °C, namely,  $2600\text{ M}^{-1}$  and  $4100\text{ M}^{-1}$  for the  $\text{Pd}^{2+}$  and  $\text{Pt}^{2+}$  receptors, respectively. Solvent effects in controlling host–guest stability have been considered before.<sup>[16]</sup> The solvent factors controlling host–guest stability can be delineated by the thermodynamic cycle shown in Scheme 1. The free energy of host–guest formation in solution,  $\Delta G_s^{\text{H,G}}$ , is enhanced by the solvation energy of the host–guest complex,  $\Delta G_{\text{gs}}^{\text{H}}$ , and by the intrinsic (gas phase) stability,  $\Delta G_g^{\text{H,G}}$ , but formation is inhibited by the solvation energies of the host,  $\Delta G_{\text{gs}}^{\text{H}}$ , and of the guest,  $\Delta G_{\text{gs}}^{\text{G}}$ .

Thus, for example, the stability of a host–guest adduct in water will be high when a hydrophobic guest is used. Many of the host–guest complexes reported by Fujita<sup>[17]</sup> rely on the hydrophobic character of the guests that are incarcerated into water-soluble receptors.

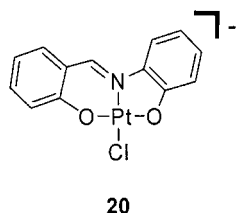
Aside from solvation effects, the stabilities of the host–guest complexes described using 9-MA as a guest are probably controlled by two factors.<sup>[1]</sup> One is  $\pi$ – $\pi$  interactions and



Scheme 1.

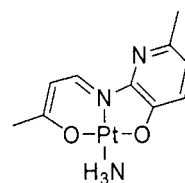
the other may involve charge-induced dipole effects, the charge being that carried by the terpy-M-Ligand units. The interplanar separations between the guest in the cleft and the terpy-M-Cl units of the receptor are found to be 3.44 and 3.48 Å (Figure 3), essentially those expected for  $\pi$ - $\pi$  stacking (3.45 Å).<sup>[18]</sup> For the case of the 1:1 adduct between the  $\text{Pt}^{2+}$  receptor and **19**, the separation between the planes of terpy-Pt-Cl units and **19** in the cleft are quite short, 3.286 and 3.271 Å, indicating that the Pt-Pt bonding leads to contraction of the distances from that expected for only  $\pi$ - $\pi$  stacking.

**Electrostatic Interactions:** Electrostatic attraction can also be used for host-guest formation.<sup>[19]</sup> The  $\text{Pd}^{2+}$  and  $\text{Pt}^{2+}$  dicationic receptors, **1**,  $\text{X} = \text{Cl}$ , form very insoluble products when their solutions are mixed with solutions of anionic planar complexes, as noted earlier. The potential guest, **20**, however, can be induced to form 1:1 host-guest crystals with **1**,  $\text{Pd}^{2+}$ ,  $\text{X} = \text{Cl}$  and with  $\text{PF}_6^-$  as the counterion.<sup>[20]</sup> The guest, **20**, lies within the cleft and the two terpy-Pd-Cl planes and that of the guest are parallel with separations of 3.21 and 3.29 Å, which are much shorter than those found for  $\pi$ - $\pi$  interactions. The short spacings appear to be due to electrostatic attraction rather than to metal-metal bonding because the metal-metal distances are 4.0, 4.7 Å, distances much too large for metal-metal bonding.

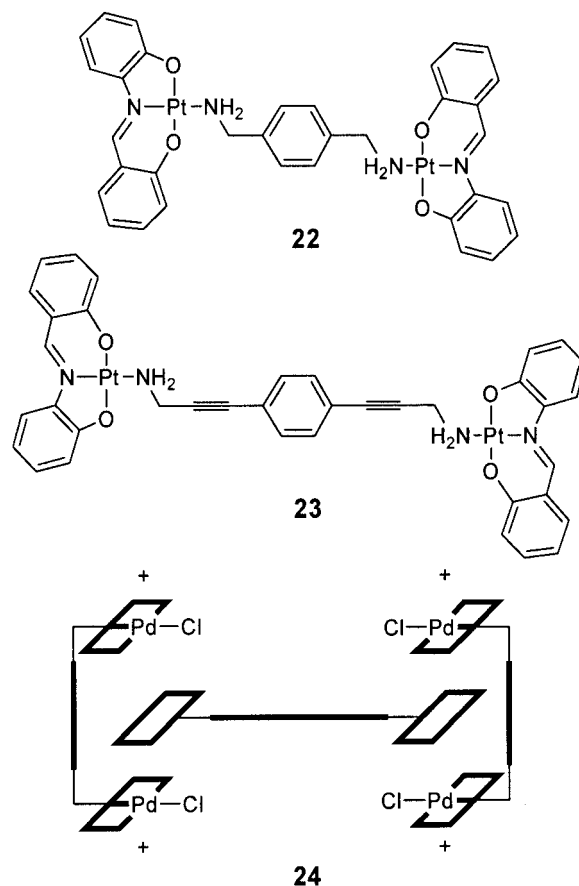


The potential guest **21** resembles **19**, but unlike **19** it carries a (free) basic nitrogen atom that can be protonated. Using the  $\text{Pd}^{2+}$  receptor **1**,  $\text{X} = \text{Cl}$ , in acetonitrile solutions at 70 °C, **21** forms a stable, red 1:1 complex ( $K = 21000 \text{ M}^{-1}$ ).<sup>[8]</sup> Sequential addition of trifluoroacetic acid to an acetonitrile solution of 1:1 host-guest adduct progressively leads to dissociation of the guest, which is accompanied by the loss of the red color. Addition of sufficient base ( $\text{Et}_3\text{N}$ ) to such acidified solutions leads to the complete restoration of the adduct (and the red color). The

proton-induced dissociation of the guest appears to be controlled by electrostatic repulsion between the cationic receptor and the cationic protonated guest (The nitrogen atom of the spacer is not protonated under the conditions). Thus, electrostatics can be used to control host-guest adduct formation. As noted in our paper,<sup>[8]</sup> the protonmotive dissociation of the guest can be described in terms of the mechanisms by which molecular motors operate<sup>[21,22]</sup> although the simple one-stroke process can hardly be described as a motor. However, studies in this area are a prerequisite to designing synthetic molecular motors, machines and switches.



We present one final example where electrostatics appears to play a role in host-guest formation but it is of an unconventional kind. Using the two ditopic guests **22** and **23**, and the  $\text{Pd}^{2+}$  receptor **1** ( $\text{X} = \text{Cl}$ ), it was considered possible to form the assembly **24**.<sup>[23]</sup> The two ditopic guests





are derivatives of **19** and hence 2:1 host–guest adducts of the kind **24** are expected to form. Molecular models indicate that there are no steric impediments to the formation of the structure **24** with either **22** or **23**, where the closest Pt...Pt distances between receptors are 12.2 and 18.8 Å, respectively.  $^1\text{H}$  NMR titration of the  $\text{Pd}^{2+}$  receptor with the two ditopic guests **22** and **23** in  $[\text{D}_7]\text{DMF}$  solutions at 70 °C, shows that **22** forms a 1:1 host–guest adduct ( $K = 1100 \pm 100 \text{ M}^{-1}$ ) but with the longer guest **23** a 2:1 host–guest complex is formed ( $K_1 = 1000 \pm 100 \text{ M}^{-1}$ ,  $K_2 = 400 \pm 50 \text{ M}^{-1}$ ), all  $K$ s are microscopic constants. The negative cooperativity observed with the longer guest **23**, and the extreme case of negative cooperativity seen with the shorter guest **22** suggests that the most likely source of the negative cooperativity is electrostatic repulsion between the two receptor molecules.<sup>[23]</sup> Approximate electrostatic calculations<sup>[23]</sup> give results consistent with the host–guest stoichiometries observed.<sup>[23]</sup>

By the observation of a 1:1 adduct formed between **22** and the  $\text{Pd}^{2+}$ -based molecular rectangle derived from linker **6** it was demonstrated that the shorter ditopic guest can form adducts with two receptor units. The equilibrium constant was found to be  $K^{\text{DMF}}_{70\text{ °C}} = 1500 \pm 200 \text{ M}^{-1}$ .

**Structure of the Molecular Spacer:** The structure of the molecular receptors incorporates important characteristics necessary for the incarceration of the guests in the cleft. As we have noted, the cofacial terpy-M–X units can rotate about the single bonds of the spacer, so that the separation between the terpy-M–X units can be adjusted to optimize the cleft separation for the guest. The result of the concerted rotation of the terpy-M–X unit about the spacer is that the mean molecular plane of the spacer is tilted with respect to the terpy-M–Cl planes. This is illustrated by the “front” view of the structure of the host  $[\text{1-Pt}^{2+}(\text{X} = \text{Cl})](\text{SbF}_6)_2$ , with the guest, **19** (Figure 7).

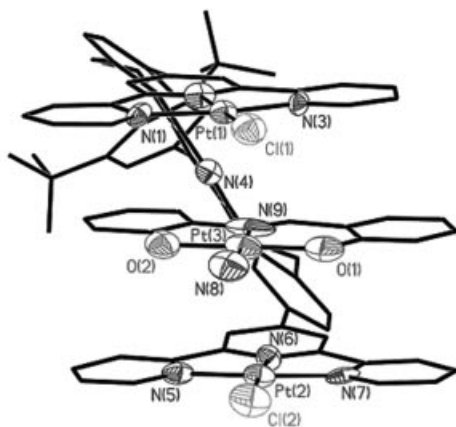


Figure 7. A “front view” of the host–guest complex,  $[\text{1-Pt}^{2+}(\text{X} = \text{Cl})]^{2+}(\text{SbF}_6)_2 \cdot \text{19}$ . Note that the mean molecular plane of the spacer is tilted with respect to the terpy-M–Cl and the guest, **19**, planes which are essentially parallel. The tilt of the spacer with respect to the terpy-M–Cl and **19** planes is 42°. Solvent and counterions have been removed for clarity. Thermal ellipsoids are shown at 50% probability.

In addition to terpy-M–X unit rotations, the spacer in all of the crystal structures determined exists in the racemic conformation. The racemic conformation of the spacer causes the M–X vectors of the two terpy-M–X units to twist with respect to each other in a sense dictated by the absolute configuration of the spacer (Figure 7). The rate of interconversion of the puckered spacer from the racemic to the *meso* conformations is likely to be a very rapid process. The large chemical shifts of  $^{195}\text{Pt}$  NMR spectra allowed us to determine the rate of this conformational interchange.

Figure 8 shows the temperature variation of the  $^{195}\text{Pt}$  NMR in  $\text{CD}_3\text{CN}$  solution of the free  $\text{Pt}^{2+}$  receptor **1** ( $\text{X} = \text{Cl}$ ).<sup>[15]</sup> At lower temperatures two signals of roughly equal intensities are observed. These are assigned to the racemic and *meso* forms of the spacer. At higher temperature these signals coalesce. Analysis of the spectra indicates that the lifetime of any conformational state at 20 °C is about  $5 \times 10^{-4} \text{ s}$ , the enthalpy of activation is  $2.7 \text{ kcal}\cdot\text{mol}^{-1}$ , and the statistically adjusted entropy of activation is  $-34 \text{ cal}\cdot\text{mol}^{-1} \text{ K}^{-1}$ . As is evident from the two spectra of the host–guest adduct between **1**,  $\text{Pt}^{2+}$ , ( $\text{X} = \text{Cl}$ ) and **19** shown in Figure 9, rapid conformational interchange also occurs between the racemic and *meso* forms which, at 20 °C, are again approximately in equal proportions. These spectra indicate that the host–guest adduct is supported by both the racemic and *meso* forms of the host which is undergoing

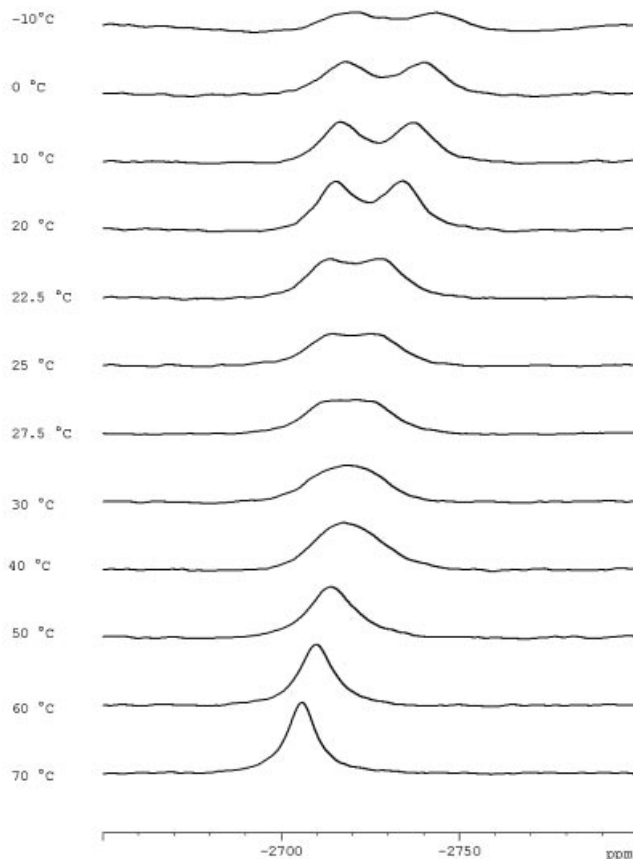


Figure 8. Variable temperature  $^{195}\text{Pt}$  NMR spectra of  $[\text{1-Pt}^{2+}, (\text{X} = \text{Cl})]^{2+}(\text{SbF}_6)_2$  in  $\text{CD}_3\text{CN}$ . The chemical shifts ( $\delta$  scale) are vs.  $\text{K}_2[\text{PtCl}_6]$  in water as an external reference.

rapid conformation interchange. Thus it is probable that our other host–guest adducts are formed with fluxional receptors.

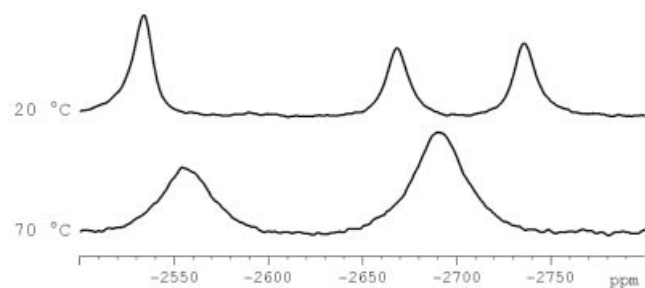


Figure 9.  $^{195}\text{Pt}$  NMR spectra of the host–guest adduct formed between  $[\mathbf{1}\text{-Pt}^{2+} (\text{X} = \text{Cl})]^{2+}(\text{SbF}_6)_2$  and **19** in  $\text{CD}_3\text{CN}$  solution ( $\delta$  scale). No Pt–Pt coupling is observed because of the broadness of the peaks. Three signals are observed for the host–guest adduct at 20 °C; the receptor shows two broad signals at  $\delta = -2669$  and  $-2736$  ppm of similar intensities and the incarcerated guest provides a signal at  $\delta = -2534$  ppm. Upon raising the temperature to 70 °C, the two receptor signals coalesce to a single peak at  $\delta = -2690$  ppm and the guest signal occurs at  $\delta = -2554$  ppm.

## Conclusions

This brief review of our studies of host–guest formation with the receptors **1**, and the molecular rectangles and trigonal prisms derived from them, serves to illustrate some of the forces that can control molecular recognition. The guest 9-MA (**15**) associates with the molecular clefts by forming 1:2 host–guest adducts so that when the clefts are incorporated in molecular rectangles or trigonal prisms, multiple guest association occurs. The forces that cause these molecular associations are probably  $\pi$ – $\pi$  interactions, supplemented by charge-induced dipole attractions. A new molecular recognition force, namely weak metal–metal bonding in  $d^8$  complexes, has been shown to add stability to host–guest formation. The strongest of the molecular recognition forces is electrostatic interaction where cationic receptors, such as **1**, do not associate with cationic guests in solution. This has been demonstrated in several ways but perhaps most persuasively by the dissociation of a neutral guest in a cationic cleft after protonation of the guest. Anionic guests form what appear to be strong complexes with the cationic receptors. Electrostatics are responsible for controlling the stoichiometry of ditopic guest interaction with the molecular clefts. An understanding of the forces that control molecular recognition form the basis for designing molecular motors, switches and machines.

## Acknowledgments

This work was supported by grants from the Basic Energy Sciences Division of the US Department of Energy.

- [1] A. J. Goshe, J. D. Crowley, B. Bosnich, *Helv. Chim. Acta* **2001**, 84, 2971.
- [2] a) S. Leininger, B. Olenyuk, P. J. Stang, *Chem. Rev.* **2000**, 100, 853; b) M. Fujita, K. Umemoto, M. Yoshizawa, N. Fujita, T. Kusukawa, K. Biradha, K. Chem. Commun. **2001**, 509; c) F. Hof, S. L. Craig, C. Nuckolls, J. Rebek, Jr., *Angew. Chem.* **2002**, 114, 1556; *Angew. Chem. Int. Ed.* **2002**, 41, 1488; d) S. R. Seidel, P. J. Stang, *Acc. Chem. Res.* **2002**, 35, 972; e) G. F. Swiegers, T. J. Malefetse, *Chem. Rev.* **2000**, 100, 3483; f) D. L. Caulder, K. N. Raymond, *Acc. Chem. Res.* **1999**, 32, 975; g) B. J. Holliday, C. A. Mirkin, *Angew. Chem.* **2001**, 113, 2076; *Angew. Chem. Int. Ed.* **2001**, 40, 2022.
- [3] R. D. Sommer, A. L. Rheingold, A. J. Goshe, B. Bosnich, *J. Am. Chem. Soc.* **2001**, 123, 3940.
- [4] The exchange rate constants for one  $\text{CH}_3\text{CN}$  ligand of the complexes,  $[\text{Pd}(\text{CH}_3\text{CN})_4]^{2+}$  and  $[\text{Pt}(\text{CH}_3\text{CN})_4]^{2+}$  in nitromethane solution at room temperature differ by  $10^5$ , where the exchange for the  $\text{Pd}^{2+}$  complex is fast but is slow for the  $\text{Pt}^{2+}$  compound. O. F. Wendt, N.-F. K. Kaiser, L. I. Elding, *J. Chem. Soc. Dalton Trans.* **1997**, 24, 4733. This difference in rates allowed us to prepare  $\text{Pt}^{2+}$  supramolecular assemblies by equilibration at higher temperatures and over longer periods than for the  $\text{Pd}^{2+}$  analogues. At ambient temperatures the  $\text{Pt}^{2+}$  assemblies are kinetically stable but the  $\text{Pd}^{2+}$  analogues are kinetically labile.
- [5] a) A. J. Goshe, B. Bosnich, *Synlett* **2001**, 941; b) J. D. Crowley, B. Bosnich, unpublished results, **2004**.
- [6] a) C. A. Schalley, T. Muller, P. Linnartz, M. Witt, M. Schafer, A. Lutzen, *Chem. Eur. J.* **2002**, 8, 3538; b) C. A. Schalley, *Mass Spectrom. Rev.* **2001**, 20, 253; c) C. A. Schalley, *Int. J. Mass Spectrom.* **2000**, 194, 11.
- [7] J. D. Crowley, A. J. Goshe, B. Bosnich, *Chem. Commun.* **2003**, 2824.
- [8] a) A. J. Goshe, PhD Thesis, The University of Chicago, **2003**; b) J. D. Crowley, A. J. Goshe, I. M. Steele, B. Bosnich, *Chem. Eur. J.* **2004**, 10, 1944.
- [9] a) A. S. Meyer, G. H. Ayers, *J. Am. Chem. Soc.* **1957**, 79, 49; b) H.-J. Schneider, *Principles and Methods in Supramolecular Chemistry*, John Wiley & Sons, New York, **2000**; c) H. Tsukube, H. Furuta, A. Odani, Y. Takeda, K. Yoshihiro, Y. Inoue, Y. Liu, H. Sakamoto, K. Kimura, *Comprehensive Supramolecular Chemistry* (Eds.: S. E. D. Davies, J. A. Ripmeester), Pergamon, Oxford, UK, **1996**, vol. 8, p. 425.
- [10] K. A. Connors, *Binding Constants*, John Wiley & Sons, New York, **1987**.
- [11] A. J. Goshe, I. M. Steele, C. Ceccarelli, A. L. Rheingold, B. Bosnich, *Proc. Natl. Acad. Sci. USA* **2002**, 99, 4823.
- [12] G. Magnus, *Pogg. Ann.* **1828**, 14, 239.
- [13] a) J. S. Miller, *Extended Linear Chain Compounds*, Plenum, New York, **1982–1983**; vols. 1–3; b) J. R. Miller, *J. Chem. Soc.* **1965**, 713; c) K. Krogmann, *Angew. Chem.* **1969**, 81, 10; *Angew. Chem. Int. Ed. Engl.* **1969**, 8, 35; d) V. H. Houlding, V. M. Misowski, *Coord. Chem. Rev.* **1991**, 111, 145; e) W. B. Connick, R. E. Marsh, W. P. Schaefer, H. B. Gray, *Inorg. Chem.* **1997**, 36, 913; f) W. B. Connick, L. M. Henling, R. E. Marsh, H. B. Gray, *Inorg. Chem.* **1996**, 35, 6261.
- [14] a) S. Yamada, R. Tsuchida, *J. Am. Chem. Soc.* **1953**, 75, 6351; b) S. Yamada, *Bull. Chem. Soc. Japan* **1951**, 24, 125; c) S. Yamada, *J. Am. Chem. Soc.* **1951**, 73, 1579; d) S. Yamada, *J. Am. Chem. Soc.* **1951**, 73, 1182.
- [15] A. J. Goshe, I. M. Steele, B. Bosnich, *J. Am. Chem. Soc.* **2003**, 125, 444.
- [16] D. B. Smithrud, S. I. Chao, S. B. Ferguson, D. R. Carcanague, J. D. Evanseck, K. N. Houk, F. Diederich, *Pure Appl. Chem.* **1990**, 62, 2227.
- [17] a) M. Fujita, *Chem. Soc. Rev.* **1998**, 27, 417; b) J.-P. Bourgeois, M. Fujita, *Aust. J. Chem.* **2002**, 55, 619; c) M. Fujita, *Acc. Chem. Res.* **1999**, 32, 53; d) M. Fujita, K. Ogura, *Coord. Chem. Rev.* **1996**, 148, 249.

- [18] a) C. A. Hunter, M. N. Meah, J. K. M. Sanders, *J. Am. Chem. Soc.* **1990**, *112*, 5773; b) C. Janiak, *J. Chem. Soc., Dalton Trans.* **2000**, 3885; c) C. A. Hunter, K. R. Lawson, J. Perkins, C. J. Urch, *J. Chem. Soc. Perkin, Trans. 2* **2001**, 651; d) E. A. Meyer, R. K. Castellano, F. Diederich, *Angew. Chem.* **2003**, *115*, 5116; *Angew. Chem. Int. Ed.* **2003**, *42*, 1210.
- [19] a) K. K. Klausmeyer, T. B. Rauchfuss, S. R. Wilson, *Angew. Chem.* **1998**, *110*, 1808; *Angew. Chem. Int. Ed. Engl.* **1998**, *37*, 1694; b) F. P. Schmidtchen, *J. Chem. Soc., Chem. Commun.* **1984**, *16*, 1115; c) M. Fujita, D. Oguro, M. Miyazawa, H. Oka, K. Yamaguchi, K. Ogura, *Nature* **1995**, *378*, 469; d) M. Aoyagi, K. Biradha, M. Fujita, *J. Am. Chem. Soc.* **1999**, *121*, 7457; e) T. N. Parac, D. L. Caulder, K. N. Raymond, *J. Am. Chem. Soc.* **1998**, *120*, 8003.
- [20] A. J. Goshe, I. M. Steele, B. Bosnich, *Inorg. Chim. Acta* **2004**, *357*, 4544.
- [21] a) V. Balzani, M. Venturi, A. Credi, *Molecular Devices and Machines*, Wiley-VCH, Weinheim, **2003**; b) V. Balzani, A. Credi, F. M. Raymo, J. F. Stoddart, *Angew. Chem.* **2000**, *112*, 3484; *Angew. Chem. Int. Ed.* **2000**, *39*, 3349.
- [22] G. Oster, H. Wang, *Molecular Motors* (Ed.: M. Schliwa), Wiley-VCH, Weinheim, **2003**, chapter 8, p. 207.
- [23] J. D. Crowley, A. J. Goshe, B. Bosnich, *Chem. Commun.* **2003**, 392.

Received: January 28, 2005  
Published Online: April 25, 2005